Optimizing Surgical Efficiency by Designing Lightweight Skull-PSI Assemblies and Curved Fixture Plates for Cranial Reconstruction using FEA

Journal:	*Part L: Journal of Materials: Design and Applications*
Manuscript ID	JMDA-24-0551.R1
Manuscript Type:	Original article
Date Submitted by the Author:	17-Dec-2024
Complete List of Authors:	Jindal, Prashant; Panjab University, Kalra, Anirudh; University Institute of Engineering and Technology, MECHANICAL Dadwal, Naveen; Panjab University, University Institute of Engineering & Technology Goel, Aparna; Panjab University, University Institute of Engineering & Technology Gupta, Vipin; Government Medical College and Hospital, Sector 32, Craniofacial Surgery Reinwald, Yvonne; Nottingham Trent University - Clifton Campus, Engineering Breedon, Philip; Nottingham Trent University, Science & Technology Juneja, Mamta; University Institute of Engineering and Technology, CSE
Keywords:	Biomaterials (also Medical Biomaterials), Materials Testing, Materials Modelling, Materials Research, Materials: Mechanical Properties/ Strength
Abstract:	Cranial reconstruction using implants is critical for protecting intracranial structures and restoring cerebral hemodynamics in cases of cranial defects caused during accidents, diseases, or cancer. Patient-specific implants(PSIs), made from materials such as polyether-ether-ketone(PEEK), are desired to be lightweight, high in strength and capable of mimicking the natural bone structure. Effective fastening mechanisms using the required number of fixture plates are essential for seamless integration between the PSI and the cavity of a defected skull for successful cranial reconstruction. This study explores the optimal number and shape of fixture plates required to join a Skull-PSI assembly, such that the overall weight of the PSI remains minimal, and this assembly does not fail when subjected to heavy external loads of 950N. PEEK material was used for PSI, natural bone for the defected skull and Titanium Alloy (Ti-6Al-4V) for the fixture plates. Conventional straight shaped fixture plates often require manual bending for proper fitment on the Skull-PSI curved surface, which increases a surgeon's time and effort. Curved shaped fixture plates were designed, to save on this time and effort, and enhance the contact surface area with the Skull-PSI surface. Four, three and two numbered, straight and curved shaped fixture plates were investigated using Finite Element Analysis (FEA) techniques. Three numbered, curved shaped fixture plates were found to be optimal, to generate a 7-gram lightweight PSI that could successfully sustain external loads up-to 950N without failure.

	Ultimately, these design improvements would benefit both patient and surgeon in aspects of time and comfort.

Optimising Surgical Efficiency by Designing Lightweight Skull-PSI Assemblies and Curved Fixture Plates for Cranial Reconstruction using FEA

Prashant Jindal[1], Anirudh Kalra[1], Naveen Dadwal[1], Aparna Goel[1], Vipin Gupta[2], Yvonne Reinwald[3,4]*, Philip Breedon[3,4]*, Mamta Juneja[1]*

[1] *University Institute of Engineering and Technology, Panjab University, Sector 25, Chandigarh, India -160014*
[2] *Government Medical College and Hospital, Chandigarh, India*
[3] *School of Science and Technology, Department of Engineering, Nottingham Trent University, Nottingham, UK*
[4]*Medical Technologies Innovation Facility, Nottingham Trent University, Nottingham, UK*

Corresponding authors: ***yvonne.reinwald@ntu.ac.uk, *philip.breedon@ntu.ac.uk, , *mamtajuneja@pu.ac.in**

Abstract

Cranial reconstruction using implants is critical for protecting intracranial structures and restoring cerebral hemodynamics in cases of cranial defects caused during accidents, diseases, or cancer. Patient-specific implants(PSIs), made from materials such as polyether-ether-ketone(PEEK), are desired to be lightweight, high in strength and capable of mimicking the natural bone structure. Effective fastening mechanisms using the required number of fixture plates are essential for seamless integration between the PSI and the cavity of a defected skull for successful cranial reconstruction.

This study explores the optimal number and shape of fixture plates required to join a Skull-PSI assembly, such that the overall weight of the PSI remains minimal, and this assembly does not fail when subjected to heavy external loads of 950N. PEEK material was used for PSI, natural bone for the defected skull and Titanium Alloy (Ti-6Al-4V) for the fixture plates.

Conventional straight shaped fixture plates often require manual bending for proper fitment on the Skull-PSI curved surface, which increases a surgeon's time and effort. Curved shaped fixture plates were designed, to save on this time and effort, and enhance the contact surface area with the Skull-PSI surface.

Four, three and two numbered, straight and curved shaped fixture plates were investigated using Finite Element Analysis (FEA) techniques. Three numbered, curved shaped fixture plates were found to be optimal, to generate a 7-gram lightweight PSI that could successfully sustain external loads up-to 950N without failure.

Ultimately, these design improvements would benefit both patient and surgeon in aspects of time and comfort.

Keywords patient-specific implants, von Mises stresses, finite element analysis, polyether-ether-ketone, Ti-6Al-4V, reconstruction

1. Introduction

Cranioplasty is the process of inserting an implant material (bone or non-biological materials such as metal or plastic plates) to repair a skull vault defect that is commonly followed in neurosurgery.[1] Protecting the brain within the skull and aesthetics are the major concerns during a cranioplasty procedure.[2] Cranioplasty is used as a therapeutic tool to manage changes in Cerebrospinal Fluid (CSF), blood flow, and the metabolic needs of the brain, in addition to acting as a physical barrier to protect cerebral structures and cosmetically remodel a cranial bone defect.[3] A cranial bone defect could develop as a result of trauma, infection, tumor invasion, or when autogenous bone is unsuitable for replacement following a decompressive craniectomy because of brain haemorrhage or infarction. Traditionally, skull abnormalities have been repaired using materials such as animal bone, precious metals, autologous bone transplants, and methyl methacrylate. Traditionally, orthopaedic implants were constructed of cast or forged metal, which is significantly stiffer than natural bone. Implants should mirror the stiffness and strength qualities of hard tissue.[4] Also, to match the shape of the skull, thin titanium sheets of varying thicknesses are used and screwed together.[5] The drawback of this typical approach is that it can be challenging to achieve a precision fit and curvature during large reconstructions, particularly when a cranio-facial junction is involved in the defect.[6] In vivo usage of standard Ti6Al4V implants can result in mechanical mismatches, including stress shielding.[4] In the absence of a natural bone material, an artificial implant material needs to be used, for which the material used should be radiolucent, immune to viruses, thermally inert, immune to biomechanical processes, malleable enough to completely seal faults, easily accessible, and affordable.[7] External loads on the skull could often lead to rupture and breakage of an artificial implant material. Ti-6Al-4V-based implant materials with an elastic modulus of 115 GPa ensure that implants could resist heavy external loads.[8] These biomaterial functions might include replacing organs and tissues whole or partially, improving tissue mechanics, appearance, or both, promoting the integration of tissues, offering protection against infections, hastening the healing process, or aiding in the identification of diseases or tissue damage.[9]

With advancements in digital technologies, 3D modeling and manufacturing, accurate and reliable surgical implants are being widely designed, fabricated, and used by surgeons on patients. This leads to confidence building in a surgeon towards exact implant fabrication as per his/her conception in concurrence with a patient's anatomical contour. Digital 3D technologies have enabled the development of Patient-specific implants (PSIs) that have been widely used for surgical correction of congenital, post-traumatic, or post-surgical abnormalities.[10] In-operative fabrication techniques are avoided by PSI, which may enhance surgical workflow effectiveness and outcomes.[11]

Polyether-ether-ketone (PEEK) has been widely used as spinal PSI material including cages, rods, and screws to maintain stability in the spine so that the bones could fuse together gradually.[12] PEEK spinal fusions can prevent serious problems of stress shielding and vertebral collapse typically encountered by metallic materials. PEEK can also be used to fabricate PSIs for reconstructing maxillofacial deformities.[13] When considering application-specific performance, there isn't much space for a generic framework, but there are still certain guidelines that may be issued. In the future, the capacity to support, stimulate, and improve tissue regeneration will be the main criteria for biomaterials. When it comes to prolonging PSI longevity and promoting patient recovery, a biomaterial's level of functionality determines how much better it is than currently used biomaterials.[14] PEEK-based PSIs demonstrate superior clinical efficacy in restoring the shape of damaged structures during reconstructions.[15] With the advent of Additive Manufacturing (AM) and PEEK being a material compatible with AM, biomedical applications have been significantly assisted for fabricating complex structures.[16] Computed Tomography (CT) images of a deformity are required for designing the PSIs that could further be reproduced using AM. Traditional metal PSIs made of Ti-6Al-4V suffer from the "stress shielding" drawback, as they have a much larger elastic modulus than natural bone, which is joined with the metal PSI during any reconstruction procedure. This could lead to loosening of the PSI and ultimately its failure. Due to these reasons, selecting a PSI material such as PEEK (which has similar biomechanical properties to natural human bone) would alleviate the reconstruction procedures from such threats.[17]

Higher accuracy, improved stability, predicted outcomes, and custom shape design are some of the important benefits of digitally generated PSIs.[18] In relation to custom-made PSIs, limited challenges related to infection, foreign body reaction, and displacement have been observed.[19] For placing a PSI in conjunction with a skull bone, fixation plates are attached to keep the joint between PSI and bone reliable while performing the reconstruction procedure. Precise holes need to be drilled within the skull bone and PSI as per the fixation plate design, while micro-screws are used to fix plates with the assembly. With a dissolving point between 334°C and 343°C and a temporary use temperature of up to 300°C, PEEK is extremely tolerant to heat inside the human body. In addition to being non-toxic and easy to sterilize, it is also strong, unyielding, and safe from chemicals, fatigue, and creep.[20]

To examine the biomechanical performance of different PSI materials, the FEA approach has been well reported. Eight to ten fixation points were used with cranial PSIs and ANSYS 15 was deployed for evaluating von Mises stresses and deformations for materials like Ti-6Al-4V and PEEK.[21] PEEK material would save time-consuming alterations while simultaneously enhancing the fit, stability, and robustness of the PSI. Using Finite Element Method (FEM), Digital Imaging and Communications in Medicine (DICOM) data, which consists of images obtained from different angles of a skull, can be used to generate a 3D assembly CAD model of the damaged skull, PSI, and fixture plates.[22] The location of fixture plates on the skull-PSI interface is critical for a safe design. A fixation system should be made up of biologically inert materials, allow accurate repositioning of the bone flap between the surface of the bone flap

and the surface of the surrounding bone, be rigid and long-lasting, and should be convenient to attach.[23]

Fixture plates are used to attach a PSI with a defective skull to repair the defect with a seamless joint at the interface, by supporting the complete Skull-PSI-fixture plates assembly. The stability of a PSI relies upon the type, size, number and location of the fixture plate, such that they could sustain external loadings without failure.

Currently there are no set guidelines or recommendations for a surgeon to decide on the number, shape and location of the fixture plates while performing such a reconstruction surgery, that could save on time and effort in relation to surgical planning. A pre-planned PSI used in such a surgery needs to be optimised for minimal weight and high mechanical strength, in order to sustain external loading conditions, such that the patient could confidently restore normalcy, post this reconstruction procedure.

Therefore, a comprehensive solution to optimise the design and application of fixture plates for attaching a PSI to a defected skull during cranial reconstruction has been proposed. The study focuses on determining the optimal number, shape, and location of fixture plates and keeping the Skull-PSI-fixture plates assembly lightweight and safety against failure when subjected to heavy external loadings This solution aims to minimise a surgeon's effort and time on the operating table, streamline surgical procedures and reduce a patient's exposure to anaesthesia,[24] thereby influencing the overall surgical efficiency.

Key Contributions

- Optimised Number of Fixture Plates: Proposing optimised number of fixture plates as three that would sustain failure against external load with minimal efforts of a surgeon in fixation.
- Curved Fixture Plate Design: Demonstrates the benefits of curved fixture plates over conventional straight designs by eliminating the need for manual bending, thereby reducing the surgeon's operative time and effort.
- Lightweight PSI Design: Utilises density-based optimisation to develop lightweight PSIs that maintain the requisite mechanical strength to withstand external loading without failure.
- Improved Surgical Efficiency: Streamlines the installation of fixture plates and assembly of PSIs, reducing overall surgical time and anaesthesia exposure for patients.

2. Materials and Methods

A patient with severe brain injury resulting from a car crash underwent cranial excision at Government Medical College and Hospital (GMCH), Sector-32, Chandigarh, India. For cranioplasty, a CT scan was conducted using the Philips Ingenuity 64-slice CT machine. Various design options for Skull-PSI assembly were analysed to determine the most suitable number and shape of fixture plates attachment and location on the interface. Figure 1 illustrates the process with steps for generating cranial reconstruction models from digital CT scan data,

including suitable fixture configurations using ANSYS simulations.[22] First, a CT scan of a patient's defected skull is obtained and transformed into a DICOM format. Volume rendering and segmentation methods are used to handle these data for defect visualization and reconstruction. A Standard Tessellation Language (STL) file format is supplied with the acquired data for 3D modeling. A Skull-PSI-fixture plates assembly is then made, which includes different numbered and shaped fixture plates. These fixture plates were proposed in two shapes: straight and curved.

Further this assembly was investigated for different number of fixture plates as four, three and two for both fixture shape options, to evaluate the optimal Skull-PSI-fixture plates assembly design that would be able to resist external loads without failure.

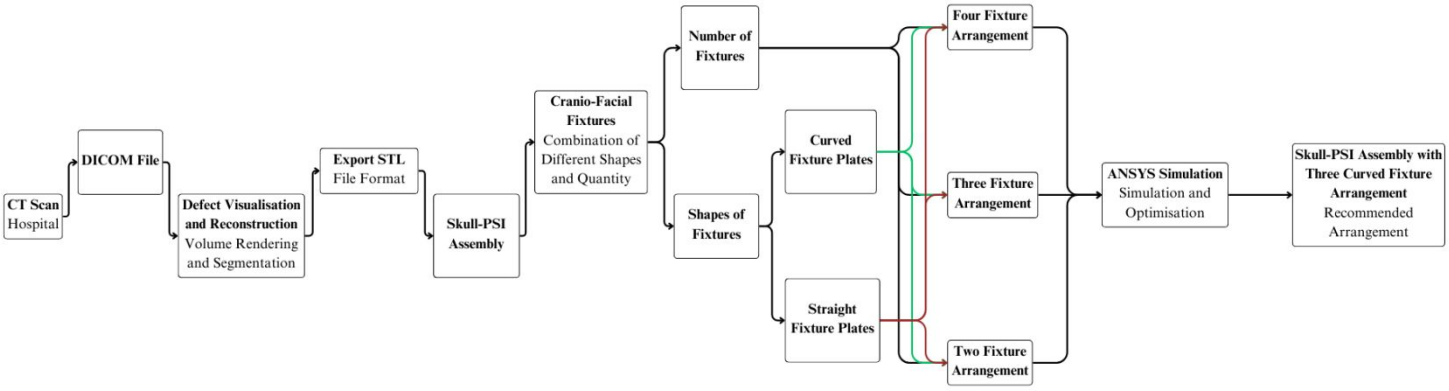

Figure 1: Methodology for generating cranial reconstruction model using digitized CT images

CT images of the patient, in DICOM format, were used for planning the PSI. A 3D assembly CAD model of the defected skull, including the PSI and fixture plate system, was developed using FEM. The boundary conditions considered were an Intracranial Pressure (ICP) of 15 mmHg and an external force of 950 N, which is experienced by human skulls during real-world scenarios related to collision forces during trauma cases, including free falls, and road accidents.[25] An average external load of 950 N is considered as equivalent to the load applied by a ball traveling at an average speed of nearly 16 m/s.[26] This load was applied across four different directions over an evenly distributed area of approximately 3 mm^2 at the centre of the implant, as shown in Figure 2. Figure 2 shows the top view of the Skull-PSI assembly and nomenclature followed for various sides of the assembly for better understanding of loading directions during analysis.

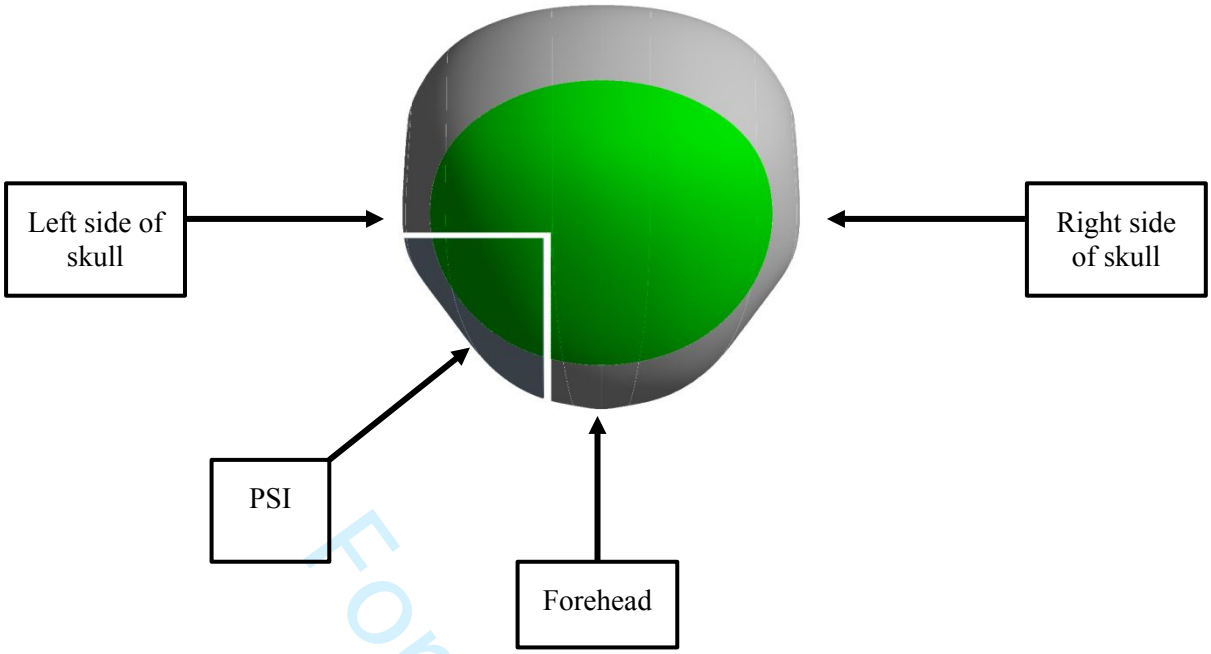

Figure 2: Nomenclature of sides from the top view of the Skull-PSI assembly

2.1 Finite Element Method (FEM)

2.1.1 Defected Skull model

The data for the patient's skull was provided in a DICOM file, in which CT scans of the patient's skull were presented in a large dataset of 2D images. These 2D images needed to be converted into a 3D model for further study. Therefore, the DICOM files were imported into an open-source software called 3D Slicer, where the first step was to volume render using a CT bone profile.[27] After volume rendering, a threshold was set to differentiate between the skull bone, tissues, and noise. This model was used to investigate the fault in three dimensions in order to fully comprehend the situation. Then, the three DICOM file views (axial, sagittal, and coronal) were utilized to determine the optimal geometry for analysing the entire cranial defect.[28] After applying volume rendering, segmentation, and surface smoothing, the skull generated was in the form of a STL file. This STL file was used to create a solid model in Autodesk Fusion. A 3D model of the defected skull based on a CT scan was exported in Standard for the Exchange of Product Data (STEP) format, as shown in Figure 3(a).

2.1.2 Generation of Patient-Specific Implants (PSI)

The defected skull was then imported into Mesh Mixer, an open-source software used to reform the missing parts of the skull. In Mesh Mixer, the defected side of the skull was first mirrored with the non-defected side, using centre of the skull as the reference axis. Then, using the Boolean command, an isolated model of the PSI was generated. Techniques to remove any sharp edges, holes, uneven shapes, and non-functional portions were applied, and smoothening

was done to complete the process, resulting in a final PSI, as shown in Figure 3(b). The file was then exported in STL format for assembly with the defected skull.

Natural human bone material properties were considered for modeling the defected skull, whereas PEEK material properties were considered for PSI. PSI materials other than autologous human bone used for cranial defect repair and reconstruction must possess properties such as biocompatibility, sufficient mechanical strength and lightweight. Ti-6Al-4V has been one of the most reliable alternative materials used for such applications. However, due to certain limitations of Ti-6Al-4V such as stress shielding effect, emission of toxic ions causing osteolysis and allergenicity, and incompatibility with CT and Magnetic resonance imaging (MRI), its mass and long-term stability within the body, other materials such as PEEK are being widely explored for fabrication of PSIs.[29] PEEK has a porous structure, which enhances its load-sharing properties.[30] If this PEEK based PSI could be optimised for lightweight and reduced stresses, then it could have wider applications and demand for the benefit of patients. Figure 3(c) shows the Skull-PSI assembly that would be further used for fixture plate attachment to complete the assembly for further analysis.

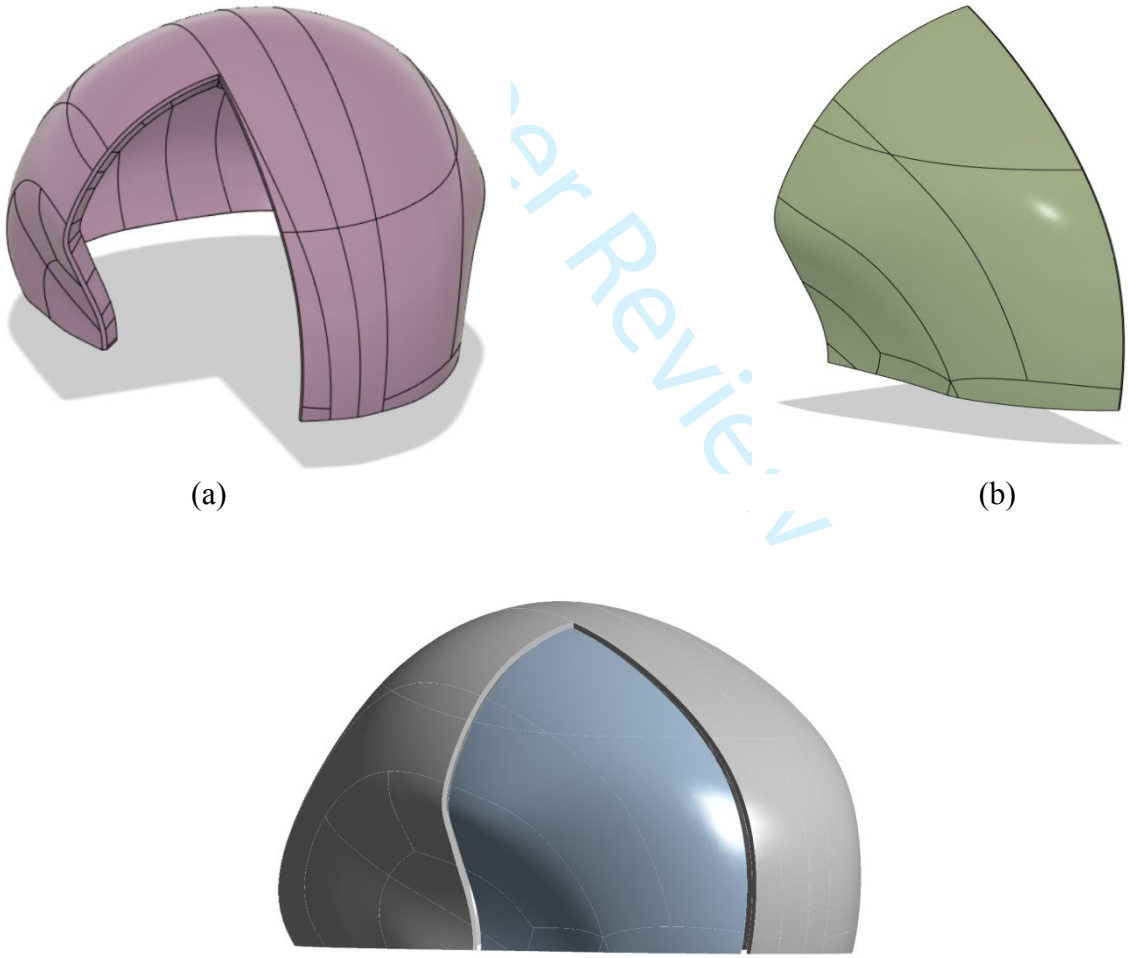

Figure 3: 3D model of (a) defected skull (b) PSI (c) Skull-PSI assembly

2.1.3 Fixture plate design and assembly

For a stable Skull-PSI integration, fixture plates need to be joined across the interface, which would keep the whole assembly safe when subjected to heavy external and internal loads. The simplest shape for fixture plates is linear, and in this study for the sake of simplicity in design and ease of handling, a linear design for the fixture plates was selected as shown in Figure 4, which will be termed as straight fixture plate for ease of understanding and comparison with other fixture plate designs.

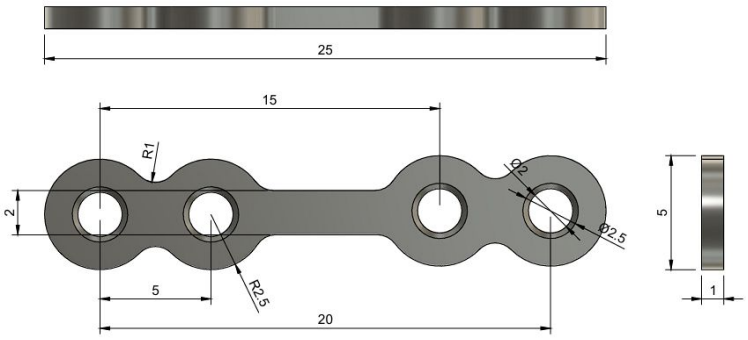

Figure 4: Different views of a straight shaped fixture plate (all dimensions in mm)

A straight fixture plate would be easier to deform or bend due to the presence of a single plate surface, to confirm the irregular or curved surfaces of a skull and PSI.[31, 32] To achieve proper mating of the skull and PSI, their surfaces are chosen to be curved, due to which it could be important to provide curvature to fixture plates also, as this would increase the contact surface area at the interface. An increased surface area would provide larger surface contact and hence could strengthen the overall assembly against failures.

Therefore, a curved fixture plate was also designed, as shown in Figure 5. These plates have been formed to a curvature shape prior to being used in assembling the skull and PSI. It is expected that due to this curved design, a surgeon would have ease of assembly both in terms of time consumption and his/her manual effort that was being consumed in bending the straight fixture plates. Ti-6Al-4V material was selected for the fixture plates due to their ease of availability and high mechanical strength.[8]

Table 1 shows the properties of materials used for various components used in this assembly. Cylindrical pins as shown in Figure 6, were used to attach fixture plates with the PSI and skull assembly. Pins were preferred over screws for simplicity[33] in design and application. The material for the pins was also considered as Ti-6Al-4V.

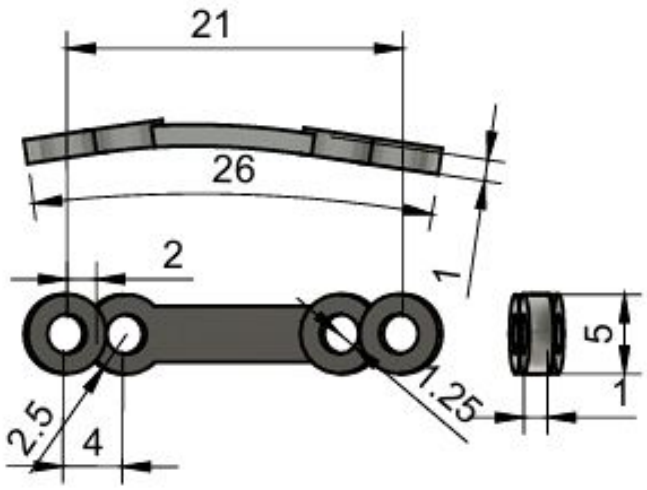

Figure 5: Different views of curved shaped fixture plate (all dimensions in mm)

Figure 7 shows the skull-implant-fixture plate assembly with the attachment of pins through the holes in fixture plates and it was ensured that they do not penetrate through the skull and PSI thickness to prevent any tissue damage within the skull. The pins provide a rotation-free fit that prevent sliding when stress is applied.

Table 1: Properties of materials used in the assembly [21, 34]

Material (component)	**Density (kg/m^3)**	**Elastic Modulus (MPa)**	**Poisson's Ratio**	**Yield Strength (MPa)**
Autologous Bone (defected skull)	4430	15,000	0.30	133
PEEK (PSI)	1240	4,000	0.44	100
Ti-6Al-4V (Fixture plate and pin)	4500	110,000	0.30	800

Four straight fixture plates were symmetrically placed at four exterior sites[8, 35, 36] as shown in Figure 7. Apart from these, two other design configurations were also generated having, three and two exterior sites. These four, three and two exterior sites were chosen to create a symmetrical arrangement and to allow uniform stress distribution throughout the PSI boundary to build a minimal support structure condition as shown in Figure 8.

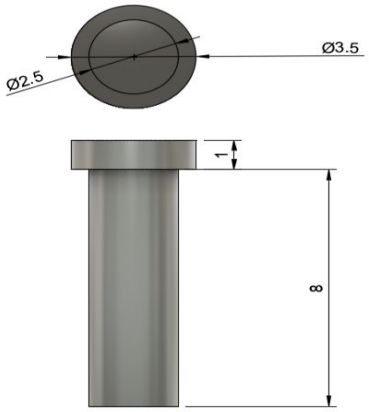

Figure 6: Cylindrical Pin used in fixation (all dimensions in mm)

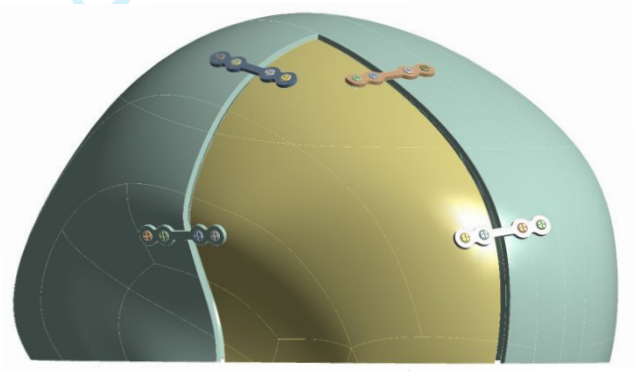

Figure 7: Skull-PSI-fixture plates assembly with four straight fixture plates

Four (Figure 8(a)) exterior sites were chosen following previous studies[8, 35, 36], while for locating three exterior sites, a symmetrical triangle was formed to place three fixture plate arrangements as shown in Figure 8(b). For locating two exterior sites, extremities of the cavity of defect were selected to form a triangle and for symmetry, mid-points of the edges of this triangle were used to place the two fixture plates, as shown in Figure 8(c).

It has been suggested that equal segmentation across the defected region could be useful in simulating a symmetrical arrangement for uniform stress distribution across the boundary of the PSI. Finally, these designs were validated by an experienced neurosurgeon.

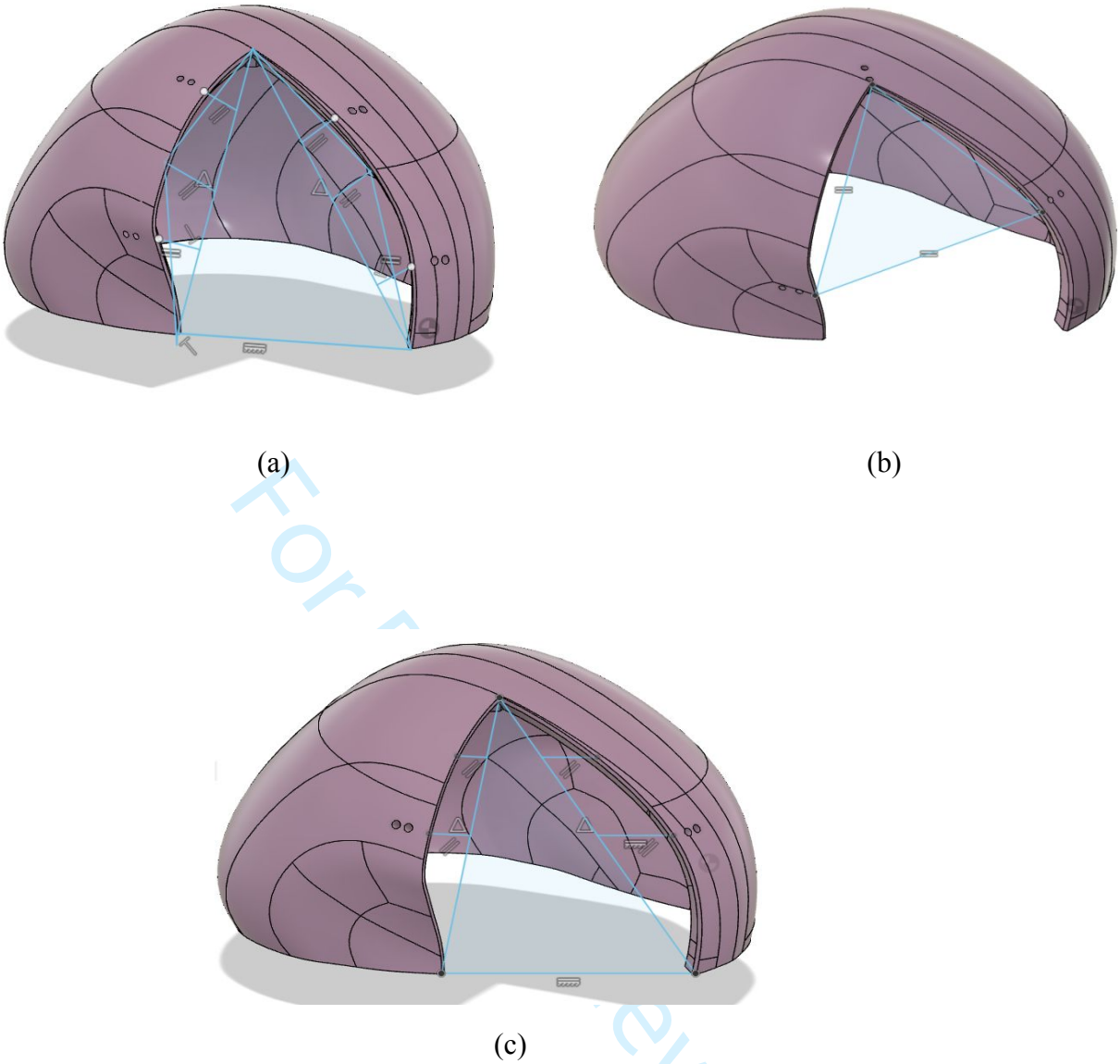

Figure 8: Exterior site locations within the defected skull having **(a)** four fixture plates (**b)** three fixture plates **(c)** two fixture plates

2.2 Finite Element Analysis (FEA)

FEA study on four, three and two fixture plates-based Skull-PSI-fixture plates assemblies was performed, using ANSYS 15 2022 R2. This was done to calculate von Mises stress (equivalent stress) on the PSI after applying external load of 950N from four different directions as top, left, right, directly on the PSI as shown in Figure 2.

2.2.1 Meshing

Using a quadratic element order and a tetrahedral element with a size of 1 mm, the span angle is fine-tuned (12°–36°) with a high smoothing factor. After applying all the properties, the

mesh was created as shown in Figure 9. The total number of nodes and elements formed in different assemblies are as shown in Table 2.

Table 2: Number of nodes and elements after meshing for various Skull-PSI-fixture assemblies having curved shaped fixture plates

Number of Fixture plates	Number of Nodes	Number of Elements
4	323590	183556
3	294141	167012
2	271044	154145

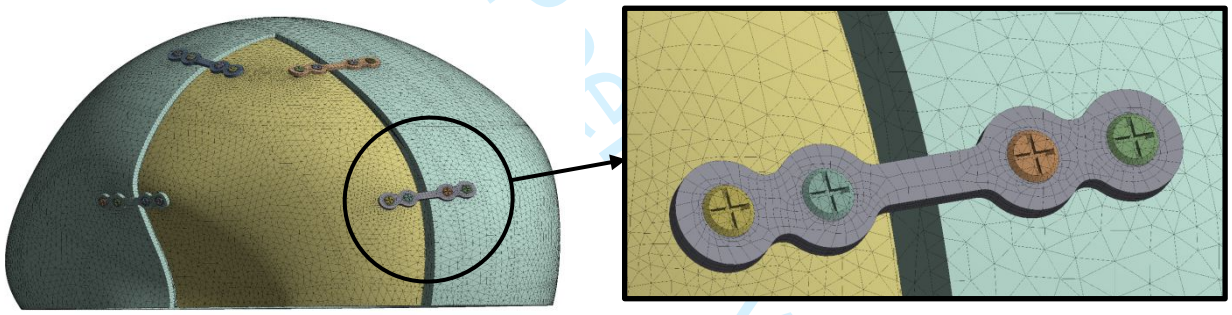

Figure 9: Meshing for Skull-PSI-fixture plates Assembly (four straight fixture plates) and across various components

2.2.2 Boundary and Loading Conditions

Several static boundary conditions, such as external load, ICP, and immobilization support, were indicated to analyse the performance of PSI and fixture plates. The combined Skull-PSI-fixture plates plate assembly was subjected to an external load[26] of 950 N, from four different directions- top of the skull, left and right sides of the skull and directly on the PSI as shown in Figure 2. The effect of this static external load from all the four directions, on various Skull-PSI-fixture plates design assemblies has been analysed for von Mises stress distribution across the PSI using FEA.

If preloading within the pins is considered as bolt pretension then[37]:

$$P = \frac{1}{FOS}(\sigma \times \frac{\pi}{4}D^2) - F \quad (1)$$

where

P is the bolted preload,
FOS is the Factor of safety
σ is the yield strength of the bolted material,
D is the diameter of the pin,
F is the external force applied

As yielding involves rapid accumulation of microdamage within the bone, safety factors for yield strain instead of ultimate failure strain of bone tissues need to be considered as 1.4 to 4.1.[38]

ICP is the pressure that fluids, including cerebrospinal fluid (CSF), exert on the brain tissue inside the skull. Age, body position, and how it affects the post-surgery skull transplant all affect it differently. For adults, the ICP should be between 7 mmHg and 15 mmHg.[8] The upper limit of ICP was used as 15 mmHg, as shown in Figure 10 (a).

A fixed support is applied to the base of the Skull-PSI-fixture plates assembly, as shown in Figure 10 (b). After defining the boundary conditions, mechanical ANSYS Parametric Design Language (APDL) was used to analyse the static structure.

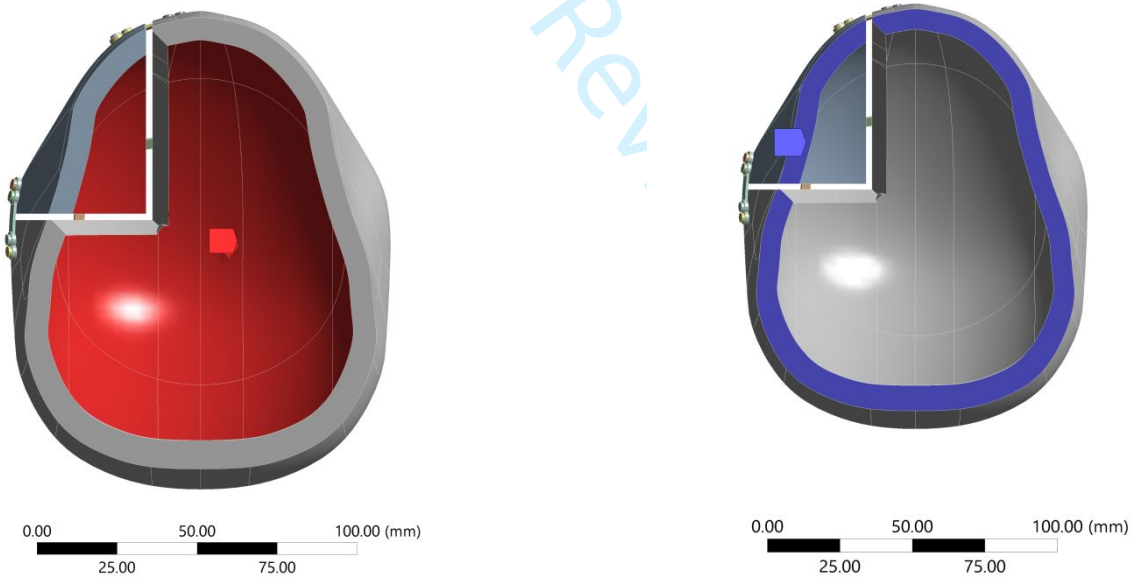

(a) (b)

Figure 10: (a) Red coloured section indicating presence of ICP (b) Blue coloured boundary showing region of immobilization support

2.3 Optimisation for mass reduction of PSI

ANSYS Mechanical structural optimisation is often utilized to decrease bulk, enhance stiffness, and decrease weight. It can also create castable structures and determine the best material distribution in a predefined design space. Based on the characteristics of the design variables, the structural optimisation model can be divided into three categories: continuous variable, discrete variable, and continuous and discrete mixed variable. In general, structural optimisation design can be classified into three levels: size optimisation, shape optimisation, and topology optimisation.[39] Here, optimisation was applied to the PSI to reduce its overall mass.

ANSYS Mechanical 2022R1 was used to apply Topology optimisation. Topology optimisation is a structural design technique that may achieve the ideal structural configuration by distributing materials uniformly while meeting the predetermined performance, load and constraint requirements.[40] There are several topology optimisation techniques such as Density-based, Level Set based and Mixable density, that explain the forms they entail using various representations. Density-based optimisation approach had been preferred, which was based on optimisation of the density of each model element. It uses Solid Isotropic Material with Penalization (SIMP), in which density was not continuously varied but was instead driven to approach 0 or 1.[41]

When the static structural analysis of the Skull-PSI-fixture plates assembly was completed, we proceeded with structural optimisation by introducing a new simulation block. First, the Design and Exclusion regions were determined, then the PSI geometry was selected for the design zone, whereas boundary criteria were used in the exclusion region, as shown in Figure 11.

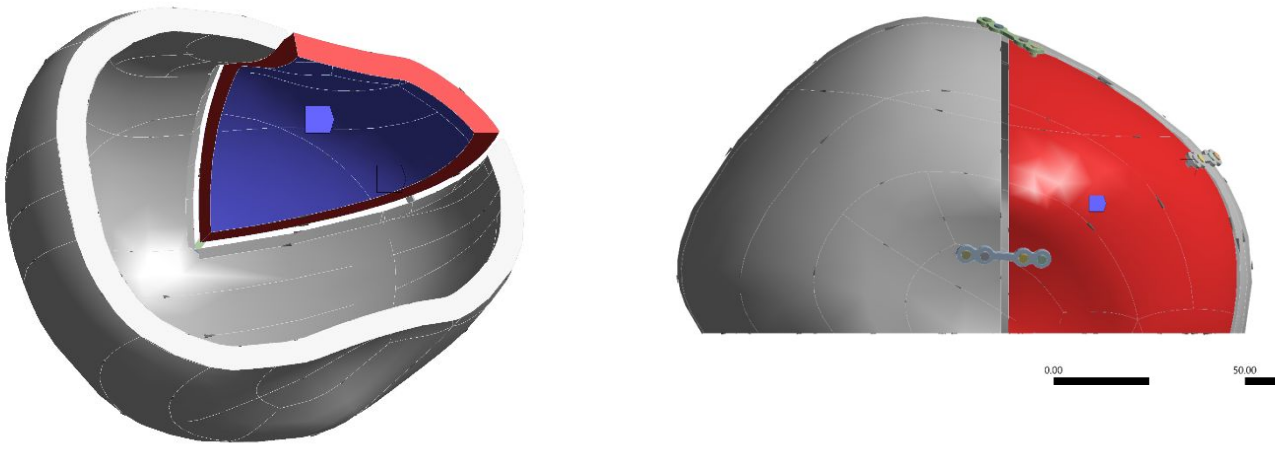

(a) **(b)**

Figure 11: (a) Design region for optimisation (b) Red portion is excluded region

Then, the objective function and response constraint were defined. In this case the minimization of the mass was the objective function. This objective is given as below

Minimize Mass

Subject to : $F(\sigma(x)) \leq 0$, $\forall x \in \Omega$ (2)

The material failure function F depends on the stress field σ (x) and strain field ε (x), and all of them are defined in an original domain Ω. Using characteristic functions to formulate (2) as an issue of material existence or non-existence results in an ill-posed problem and the possibility that there is no minimum. One potential solution to this problem is to use porous materials to include intermediate values between solids (ρ = 1) and voids (ρ = 0).[42] Out of several options, the SIMP technique, was used in this paper. Taking the relative density $0 \leq \rho \leq 1$ as the design variable[43] the constitutive behavior of the microstructure is described by relating the elasticity tensor D_ρ with the elasticity tensor of the solid material D_0 as follows:

$D_\rho = f_D(\rho) D^0 = \rho^p D^0$ (3)

With these assumptions in hand, the original problem may be written as a new one stated as

Problem P1:

$\text{Min}_{\rho \in L^\infty(\Omega;(0,1))} m(\rho) = \rho_0 \int_\Omega \rho(x)\, d\Omega$ (4)

Subject to: $\rho(x) F(\sigma(x)) \leq 0$ a.e. in Ω

Due to its applicability to a wide class of materials and to its simplicity, the von Mises failure criterion is one of the most frequently used expressions,[44] and is given by

$F_{vM}(\sigma) = (\sigma_{vM}/\sigma_{adm}) - 1$, (5)

where σ_{adm} is the material yielding stress and σ_{vM} is the effective von Mises stress. When the density reaches zero, significant deformations may occur due to the low stiffness, resulting in substantial, but finite, local stresses. The Stress-Singularity Phenomenon occurs when local restrictions saturate and lock the material-removal process.[45] Many authors reduce stress requirements, allowing for greater values as density reaches zero while still satisfying the initial limitation for solid materials.[46, 47] Then, constraints are transformed in

$g_\sigma(x) \equiv \rho(x) F(\sigma(x)) - (1-\rho(x)) \leq 0$, a.e. in Ω ,

$0 < \varepsilon^2 \leq \rho_{min} \leq \rho(x) \leq 1$, $\forall x \in \Omega$ (6)

where ε is a relaxation parameter. Taking this proposition into consideration, the problem was rewritten as

Problem P2:

$\text{Min}_{\rho \in K\rho(\Omega)} m(\rho) = \rho 0 \int_\Omega \rho(x)\, d\Omega$, (7)

Subject to: $g_\sigma(x) \leq 0$ a.e. in Ω,

where $K_\rho(\Omega)$ is the design space of density fields:

$$K_\rho(\Omega) = \{\rho \mid \rho \in L^\infty(\Omega), 0 < \varepsilon^2 \leq \rho_{min} \leq \rho(x) \leq 1\}.$$

Response constraint was set to retain firstly, (by default) 50% of mass then decrement of 10 was followed till 10% mass retention was obtained. A sequence of points on a face of the tetrahedron was generated using an active set algorithm, which solved the minimization of a quadratic function within the box constraints as mentioned above. This process continued until a minimizer of the objective function on that face or a point on the border was achieved. FEA was performed for the Skull-PSI-fixture plates assemblies in both pre and post optimisation conditions.

3. Results

A 950 N external loading was applied to various (four, three and two fixture plates) Skull-PSI-fixture plates assembly configurations across the four directions, to understand the optimal number of fixture plates for safety against failure to external loading.

3.1 Skull-PSI-fixture plates assembly with Four Straight and curved fixture plates

Deformation and von Mises stresses were calculated on the Skull-PSI-fixture plates Assembly with four straight and curved fixture plate designs as was shown in Figure 7 and Figure 12 respectively by applying forces across the four different directions.

A representative contour using FEA for such an arrangement (four curved fixture plates) has been shown in Figure 13. FEA results for von Mises stresses for both design assemblies subjected to the four external loading directions (top, left, right and directly on the PSI) have been shown in Table 3.

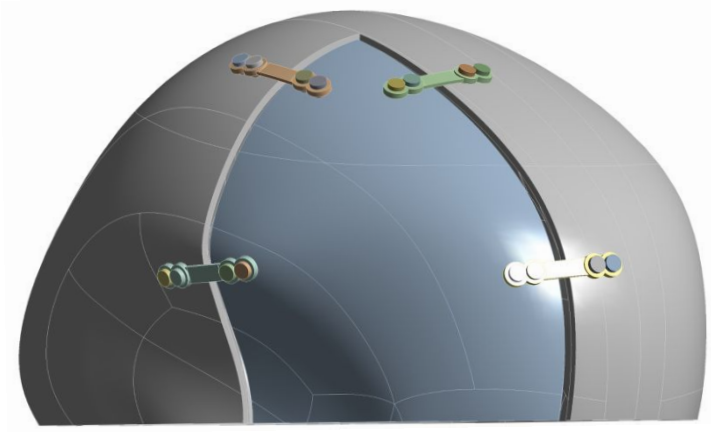

Figure 12: Skull-PSI-fixture plates assembly with four curved fixture plates

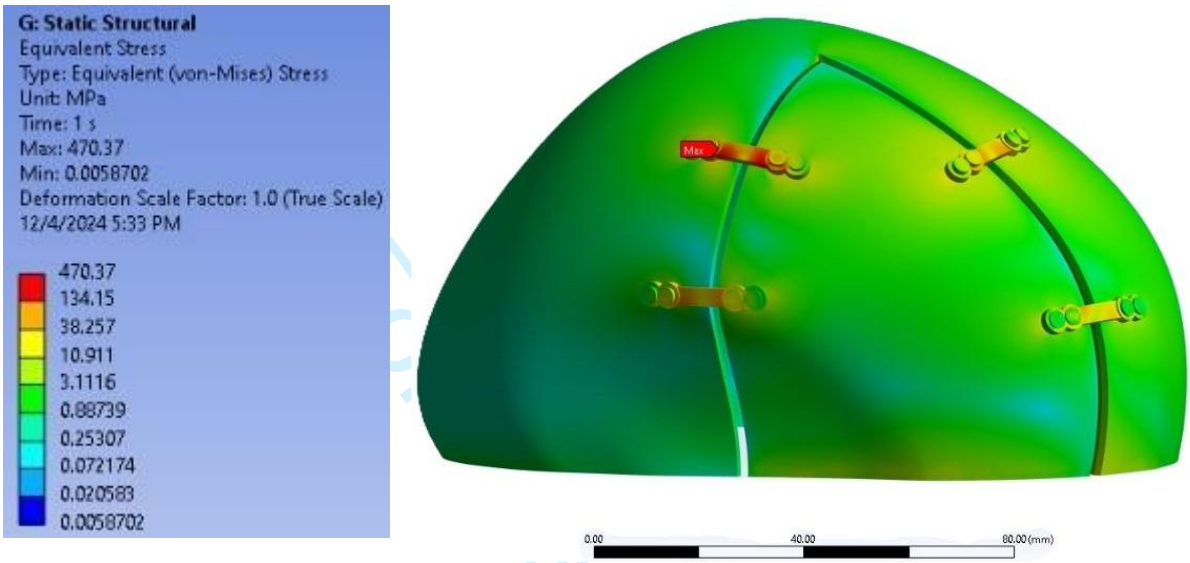

Figure 13: von Mises stress distribution on a Skull-PSI-fixture plates assembly (four curved fixture plates)

For the applied external loads, the von Mises stresses within the PSI were found to be safe and within yielding limits as shown in Table 3.

Results indicated reduced von Mises stresses within the PSI for the curved fixture plates assembly in comparison to straight fixture assembly by an average of 38.31%. Also, if bolt pretension was being considered along with external loading, then von Mises stresses within the PSI increased significantly for the curved (23.34-72.59 MPa) but remained within the yielding limits, hence no would be able to sustain external loading without failure.

For optimisation, various other design arrangements for the Skull-PSI-fixture plates assembly were then explored for three and two fixture plates, both having straight and curved plate shapes and the complete procedure for FEA was repeated.

Table 3: Equivalent von Mises stresses and reduction in % von Mises stresses between straight and curved fixture plates for Skull-PSI-fixture plates assembly with four fixture plates

Number of fixture plates	Direction of external load applied	Equivalent von Mises Stress at Maximum Deformation (MPa)		Reduction in % von Mises stresses between straight and curved fixture plates
		Straight fixture plates	Curved fixture plates	
4	Top of skull	15.97	10.96	31.35
	Left side of skull	27.25	12.85	52.86
	Right side of skull	6.98	4.32	38.04
	Directly on PSI	83.56	57.66	31.00

3.2 Skull-PSI-fixture plates Assembly with Three Straight and Curved Fixture Plates

The fixture plates in both straight and curved shapes were attached as shown in Figures 14 (a) and (b) respectively.

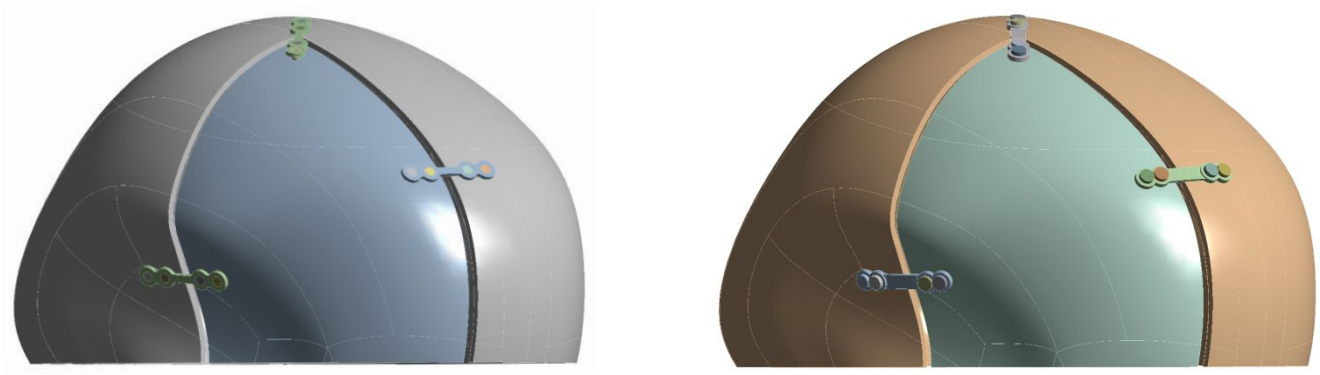

(a) **(b)**

Figure 14: Skull-PSI-fixture plates assembly with three (a) straight and (b) curved fixture plates

Table 4 shows the comparison of von Mises stresses within the PSI for these two arrangements under the same loading conditions as experienced by four Skull-PSI-fixture plates assemblies. PSI with curved fixture plates showed reduced von Mises stresses by an average of nearly 36% in comparison to PSI with straight fixture plates.

Table 4: Equivalent von Mises stresses and reduction in % von Mises stresses between straight and curved fixture plates for Skull-PSI-fixture plates assembly with three fixture plates

Number of fixture plates	**Direction of external load applied**	**Equivalent von Mises Stress at Maximum Deformation (MPa)**		**Reduction in % von Mises stresses between straight and curved fixture plates**
		Straight fixture plates	Curved fixture plates	
3	Top of skull	20.07	15.04	25.08
	Left side of skull	33.57	13.86	58.70

Number of fixture plates	Direction of external load applied	Equivalent von Mises Stress at Maximum Deformation (MPa)		Reduction in % von Mises stresses between straight and curved fixture plates
		Straight fixture plates	Curved fixture plates	
	Right side of skull	7.40	5.19	29.88
	Directly on PSI	93.35	65.03	30.33

Overall, there was an increase in stresses exhibited within the PSI, as compared to a four fixture plate assembly, however, the stresses remained within the yielding limits. Here also, if bolt pretension was being considered, then von Mises stresses within the PSI again increased significantly for the curved fixture plates (17.45-96.94 MPa), but remained marginally within the yielding limits, thereby suggesting an optimal solution for cranial reconstruction.

3.3 Skull-PSI-fixture plates Assembly with Two Straight and Curved Fixture Plates

Similar procedure was repeated for a two fixture plate assembly arrangement as shown in Figure 15 (a) and (b) for straight and curved shaped fixture plates respectively.

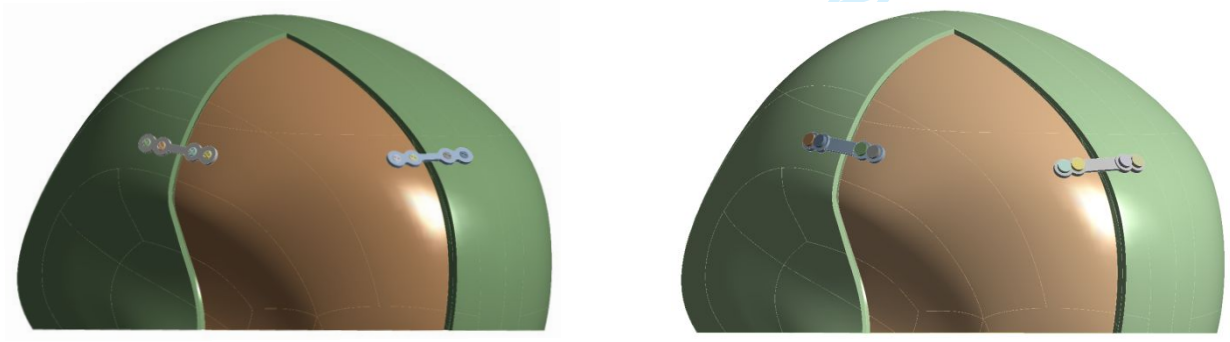

(a) **(b)**

Figure 15: Skull-PSI-fixture plates assembly with two (a) straight and (b) curved fixture plates

As the curved fixture plate design arrangement provided safer von Mises stress results for the PSI in four and three fixture plate design arrangements, a similar trend was observed for the two-fixture plate design arrangement. One fixture plate from the three-fixture design assembly was removed that experiences minimum stress and the other 2 fixture plates were adjusted to get minimum stress possible. Table 5 shows the comparison of von Mises stresses within the PSI for curved fixture plate designs for all four, three and two fixture plate design assemblies. Except for the case when the external load was directly applied on the PSI, the von Mises stresses exhibited within the PSI remained within yielding limits for two fixture plate dressing assembly also.

Overall, as expected there was an increase in stresses exhibited within the PSI, as compared to the four and three fixture plate assemblies, however, the stresses remained within the yielding limits.

Compared to the four fixture-based assemblies, stress within the PSI for three fixture assemblies increased within a range of 8% to 37% while for two fixture assemblies, this increase was within a range of 38% to 95%.

Table 5: Ratio of stresses within the PSI for two, three and four curved fixture plates Skull-PSI-fixture plates assembly when subjected to 950 N external load

Direction of external load applied	Equivalent von Mises Stress at Maximum Deformation (MPa)			Ratio of von Mises stresses for Two: Three: Four fixture plate assemblies
	Two	Three	Four	
Top of skull	18.10	15.04	10.96	1.65:1.37:1
Left side of skull	17.71	13.86	12.85	1.38:1.08:1
Right side of skull	6.02	5.19	4.32	1.39:1.20:1
Directly on PSI	112.80	65.03	57.66	1.95:1.13:1

3.4 Density-based optimisation on Skull-PSI-fixture plates assembly

Optimisation was performed to reduce deformation and stress distribution within the PSI for three and four fixture plate design assembly arrangements. During the process of density-based

or gauge optimisation and stiffness optimisation, mass retention was used to determine the mass of material to be retained. For density-based optimisation, retention was expressed as the mass percentage of the total mass of the complete design space. An optimal mass retention percentage was observed at 20%, with a reduction in mass which is equivalent to only 7 grams of PSI, that could sustain external loads without failure, as shown in Figure 16. Table 6 shows the stresses exhibited within the optimised PSI for both design assemblies.

The von Mises stress distribution is compared for each of these PSI design assemblies in Table 6. It has been observed that PSI for curved fixture plate assemblies exhibit lower stresses than their straight fixture plate counterparts, post optimisation also. Therefore, it could be suggested that curved fixture plate assemblies have always been more effective in reducing stresses within the PSI in comparison to straight fixture plate assemblies.

In addition, a three fixture plate design provides satisfactory von Mises stress results for the complete assemblies, which are preferred over four fixture plate designs as lesser number of plates, pins and drilled holes lead to saving of a surgeon's time and effort in fixation.

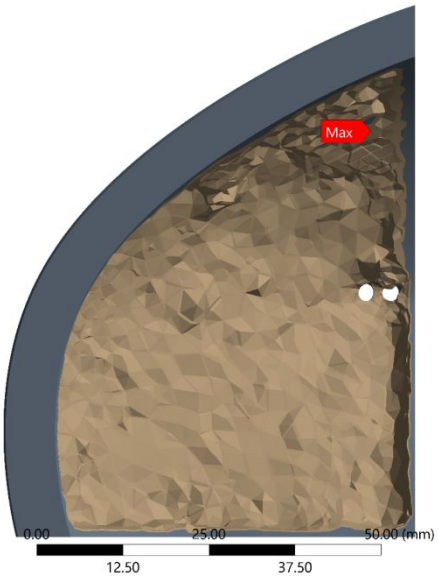

Figure 16: Optimized PSI model (with 20% mass retained)

Table 6: Ratio of stresses within the optimised PSI (7 grams mass) for three and four curved fixture plates Skull-PSI-fixture plates assembly designs subjected to 950 N external load

Direction of external load applied	Equivalent von Mises Stress at Maximum Deformation (MPa)	Ratio of stresses for

	Three fixture plates	Four fixture plates	curved fixture plates in Three: Four assemblies
Top of skull	25.891	27.89	10:11
Left side of skull	64.805	62.805	26:25
Right side of skull	4.5878	2.6733	2:1
Directly on PSI	23.871	11.522	10:5

For the three fixture plate design assembly, with the assistance of density-based optimisation, it was observed that these stresses dropped to 4.59 MPa to 64.81 MPa in comparison to the pre (5.19 MPa to 65.03 MPa as shown in Table 5) optimisation cases, within the PSI. Hence, a light weight PSI of 7 grams is able to resist a heavy external load of 950 N without mechanical failure, with the assistance of density-based optimisation is a significant finding in the domain of designing suitable Skull-PSI-fixture plates assemblies.

4. Discussion

PEEK-based PSIs have been used to reconstruct cranial defect cavities by attaching a suitable number of fixture plates across the Skull-PSI interface. Such arrangements require optimisation of the shape and number of fixture plates to minimise the PSI mass without failure under external loading, while also reducing the surgeon's effort and time in fixing these plates.

An external load of 950 N, sufficient to jeopardise a cranial reconstruction procedure, was considered and applied from four different, most probable loading directions on a Skull-PSI-fixture plates assembly. Ti-6Al-4V material was considered for the fixture plates, while autologous bone was assumed for the skull. Based on the structure of the Skull-PSI-fixture plates assembly, designs with four, three, and two fixture plates were explored and symmetrically fitted across the interface to ensure uniform stress distribution across the PSI.

Assemblies with four, three, and two straight-shaped and curved-shaped fixture plate designs were investigated using FEA to determine the von Mises stresses within the PSIs. It was observed that the curved fixture plate design provided larger surface contact support, thereby significantly reducing the stresses within the PSI compared to the straight fixture plate design. This also implied easier handling and fitment for the surgeon during the procedure, as they would not need to spend time manually bending the plate for fixation.

In comparison to the four fixture plate based design assemblies, von Mises stresses within the PSI for three fixture based assemblies increased by 8% to 37%, while for two fixture plates based assemblies, the increase ranged from 38% to 95% across various loading directions. Despite the increase, the values remained within the yielding limits of PEEK (100 MPa). However, under loading conditions directly on the PSI, the two-fixture plate design (112.8 MPa) experienced failure. Therefore, it is suggested that, under such high external loading and given the size of the skull-PSI, a two-fixture plate design may not be suitable.

A further density-based optimisation study was conducted, resulting in an optimised PSI mass of 7 grams. The corresponding FEA studies revealed that von Mises stresses within the PSI for three fixture plate design assemblies ranged from 4.59 MPa to 64.81 MPa, while for four fixture plate design assemblies, the range was 2.67 MPa to 27.89 MPa, both remaining within the yielding limits.

The presence of a larger number of Ti-6Al-4V material-based fixture plates located at critical stress concentration sites and near protruded sections, rather than coinciding with the protruded sections, is suggested as a primary factor in ensuring PSI safety against failure.48 The use of two Ti-6Al-4V material-based pins on each side of the plate provides greater stability and reduces the likelihood of failure, as compared to a single screw during major procedures.49, 50 Additionally, due to their larger surface contact area, curved fixture plates reduced stresses by nearly 36% to 38%, which could also be a significant factor. As a result of these design optimisations, a 7 gram PSI capable of sustaining 950 N external loading without failure has been successfully proposed.

5. Conclusion

Challenges in providing a lightweight, load-bearing, and biocompatible PSI for successful cranial reconstruction, ensuring patient comfort and minimal revisit still persist. In this study, a novel design approach was utilised for assembling the skull-PSI with an optimal number of fixture plates and redesigned their shapes to ensure that the overall mass of the PSI remains low. Using PEEK as the biocompatible material for the PSI instead of Ti-6Al-4V enables weight reduction, while Ti-6Al-4V is retained for the fixture plates.

The location of these fixture plates across the PSI-skull interface is critical, as it can significantly reduce von Mises stress distribution across the PSI and ensure safety against failure under heavy external loadings. It was observed that a 7-gram PSI could sustain external loading of nearly 950 N without failure, exhibiting stress ranges of 4.59 MPa to 64.81 MPa for a three curved fixture plate design assembly, and 2.67 MPa to 27.89 MPa for a four curved fixture plate design assembly. Since the yielding point of PEEK is 100 MPa, both design arrangements are considered safe. While a two curved fixture plate design assembly was also explored, its vulnerable performance under certain loading conditions suggests it may not be suitable.

Curved fixture plates play a critical role in reducing stresses (by 36% to 38% compared to straight-shaped fixture plates) due to their larger surface contact area with the PSI and skull.

Additionally, these plates save a surgeon's time and effort in bending straight-shaped plates for proper fitment. A four fixture plate design would require drilling four additional holes—two each in the skull and PSI—and placing and fitting four additional pins. Therefore, a three fixture plate design assembly is preferable, as it maintains stress levels within yielding limits while reducing complexity.

For ease of surgical planning and improved surgical efficiency, a three curved fixture plate design assembly is recommended over a four-plate design. In conventional surgery, a surgeon may spend approximately two minutes per plate bending the fixture, ten minutes per plate planning location and orientation, and one minute per hole drilling requisite holes in the PSI and skull. For surgeries involving three fixture plate systems with twelve holes (four per plate), this process can take 40 to 45 minutes in addition to the actual surgical procedure. The proposed design arrangement reduces this process to 15 to 20 minutes, as the location and curvature are pre-planned during the FEA study, and the holes can be pre-drilled in the PSI, saving additional operative time. This approach could improve overall surgical efficiency by nearly 50%, primarily by reducing time spent on location, fitment, and assembly of fixation plates.

With this significant time savings, a patient's overall exposure to anaesthesia could also be reduced, lowering the risk of unexpected allergic reactions, excessive pain, and hypoxia.

In conclusion, cranial reconstruction procedures could greatly benefit both surgeons and patients in terms of time, effort, planning, comfort, and efficiency based on the novel design findings of this study. Manual estimation of the curvature, location, and shape of a fixture plate can lead to inaccuracies and suboptimal results, as no predefined guidelines exist, leaving surgeons to rely on their experience for fitment. Design optimisation, achieved by altering the location, shapes, and number of fixation plates to reduce the overall PSI weight, could play a transformative role in planning complex reconstruction and repair procedures, especially where implant size and shape are constrained.

Acknowledgements

The authors are grateful to the Ministry of Education (MoE), Government of India, for funding this project (17-11/2015-PN-1) under the sub-theme Medical Devices & Restorative Technologies at the Design and Innovation Centre (DIC). We also acknowledge the Nottingham Trent University-Panjab University Strategic Partnership Program for funding the ANSYS 15 2022 R2 software and the Nottingham Trent University International Partnership Fund (IPF) scheme for supporting this work.

Declaration of Conflicting interests:

The author(s) declared no potential conflicts of interest with respect to the research, authorship, and/or publication of this article.

Author Contributions:

Prashant Jindal: Project administration; Conceptualization; Data investigation; Writing - review & editing; Supervision.
Anirudh Kalra: Software; Methodology; Formal analysis; Visualization.
Naveen Dadwal: Software; Formal analysis; Data visualization.
Aparna Goel: Software; Writing - original draft.
Vipin Gupta: Problem formulation; Clinical assessment.
Yvonne Reinwald: Manuscript editing and reviewing.
Philip Breedon: Manuscript editing and reviewing.
Mamta Juneja: Methodology; Formal analysis; Validation; Writing - original draft; Supervision; Project administration.

Data availability statement:

Data could be shared to the reader as per request.

References:

1. Andrabi S, Sarmast A, Kirmani A, Bhat A. Cranioplasty: Indications, procedures, and outcome - An institutional experience. Surg Neurol Int. 2017;8(1).

2. Moin H, Mohagheghzadeh P, Darbansheikh A. The Use of Frozen Autogenous Bone Flap for Cranioplasty [Internet]. Vol. 10, Journal of Research in Medical Sciences. Available from: www.mui.ac.ir

3. Alkhaibary A, Alharbi A, Alnefaie N, Oqalaa Almubarak A, Aloraidi A, Khairy S. Cranioplasty: A Comprehensive Review of the History, Materials, Surgical Aspects, and Complications. World Neurosurg [Internet]. 2020;139:445–52. Available from: https://www.sciencedirect.com/science/article/pii/S1878875020309219

4. Vance A, Bari K, Arjunan A. Investigation of Ti64 sheathed cellular anatomical structure as a tibia implant. Biomed Phys Eng Express [Internet]. 2019 Mar 12 [cited 2024 Dec 6];5(3):035008. Available from: https://iopscience.iop.org/article/10.1088/2057-1976/ab0bd7

5. Oldani C, Dominguez A. Titanium as a Biomaterial for Implants. In: Recent Advances in Arthroplasty. InTech; 2012.

6. Sundseth J, Berg-Johnsen J. Prefabricated Patient-Matched Cranial Implants for Reconstruction of Large Skull Defects. J Cent Nerv Syst Dis. 2013 Jan;5:JCNSD.S11106.

7. Shah AM, Jung H, Skirboll S. Materials used in cranioplasty: A history and analysis. Neurosurg Focus. 2014;36(4).

8. Jindal P, Chaitanya, Bharadwaja SSS, Rattra S, Pareek D, Gupta V, et al. Optimizing cranial implant and fixture design using different materials in cranioplasty. Proceedings of the Institution of Mechanical Engineers, Part L: Journal of Materials: Design and Applications. 2023 Jan 1;237(1):107–21.

9. Arjunan A, Baroutaji A, Praveen AS, Robinson J, Wang C. Classification of Biomaterial Functionality. In: Encyclopedia of Smart Materials. Elsevier; 2021. p. 86–102.

10. Mukul SK, Mishra M, Singh G, Singh A, Das MK. Patient-Specific Implants in Maxillofacial Reconstruction: A Case Report. The Traumaxilla. 2019 Dec;1(2–3):76–80.

11. Thayaparan GK, Lewis PM, Thompson RG, D'Urso PS. Patient-specific implants for craniomaxillofacial surgery: A manufacturer's experience: Custom CMF surgery: 4120 cases. Annals of Medicine and Surgery. 2021 Jun 1;66.

12. Kurtz SM, Devine JN. PEEK biomaterials in trauma, orthopedic, and spinal implants. Biomaterials [Internet]. 2007 Nov;28(32):4845–69. Available from: https://linkinghub.elsevier.com/retrieve/pii/S0142961207005467

13. Oh J hyeon. Recent advances in the reconstruction of cranio-maxillofacial defects using computer-aided design/computer-aided manufacturing. Vol. 40, Maxillofacial Plastic and Reconstructive Surgery. Springer; 2018.

14. Arjunan A, Baroutaji A, Robinson J, Praveen AS, Pollard A, Wang C. Future Directions and Requirements for Tissue Engineering Biomaterials. In: Encyclopedia of Smart Materials. Elsevier; 2021. p. 195–218.

15. Chepurnyi Y, Chernogorskyi D, Kopchak A, Petrenko O. Clinical efficacy of peek patient-specific implants in orbital reconstruction. J Oral Biol Craniofac Res. 2020 Apr 1;10(2):49–53.

16. Ahangar P, Cooke ME, Weber MH, Rosenzweig DH. Current biomedical applications of 3D printing and additive manufacturing. Vol. 9, Applied Sciences (Switzerland). MDPI AG; 2019.

17. Mallya PK, Juneja M. Rapid prototyping of orthopedic implant materials for cranio-facial reconstruction: A survey. In: Materials Today: Proceedings. Elsevier Ltd; 2021. p. 5207–13.

18. Owusu JA, Boahene K. Update of patient-specific maxillofacial implant. Current opinion in otolaryngology & head and neck surgery [Internet]. 2015 Aug;23(4):261—264. Available from: https://doi.org/10.1097/MOO.0000000000000175

19. Alasseri N, Alasraj A. Patient-specific implants for maxillofacial defects: challenges and solutions. Maxillofac Plast Reconstr Surg. 2020 Dec 1;42(1).

20. Mbogori M, Vaish A, Vaishya R, Haleem A, Javaid M. Poly-Ether-Ether-Ketone (PEEK) in orthopaedic practice- A current concept review. Journal of Orthopaedic Reports. 2022 Mar;1(1):3–7.

21. Bogu VP, Ravi Kumar Y, Khanara AK. Modelling and structural analysis of skull/cranial implant: Beyond mid-line deformities. Acta Bioeng Biomech. 2017;19(1):125–31.

22. Juneja M, Chawla J, Dhingra G, Bansal I, Sharma S, Goyal P, et al. Analysis of additive manufacturing techniques used for maxillofacial corrective surgeries. Proc Inst Mech Eng C J Mech Eng Sci. 2022 Jul 1;236(14):7864–75.

23. Piccirilli M, Spena G, Marchese E, Tropeano MP, Santoro A. A new device for bone cranial flap fixation: Technical note and surgical remarks. A multicentric experience. Surg Neurol Int. 2021 Feb 1;12.

24. D'Eramo EM, Bontempi WJ, Howard JB. Anesthesia Morbidity and Mortality Experience Among Massachusetts Oral and Maxillofacial Surgeons. Journal of Oral and Maxillofacial Surgery. 2008 Dec;66(12):2421–33.

25. Ganatsios SS, Maropoulos S, Tsouknidas A, Papanikolaou S. Porosity - Mechanical Behaviour Correlation in Cranial Implants. In 2011.

26. Tsouknidas A, Maropoulos S, Savvakis S, Michailidis N. FEM assisted determination cranial implants' mechanical strength properties. In: IFMBE Proceedings. 2010. p. 1487–90.

27. Gill DK, Walia K, Rawat A, Bajaj D, Gupta VK, Gupta A, et al. 3D modelling and printing of craniofacial implant template. Rapid Prototyp J. 2019 Feb 25;25(2):397–403.

28. Jindal P, Bhattacharya A, Singh M, Pareek D, Watson J, O'connor R, et al. Unilateral cranial defect bone reconstruction utilising 3D design and manufacturing. Transactions on Additive Manufacturing Meets Medicine Trans AMMM. 2022;4(1).

29. Jindal P, Bharti J, Gupta V, Dhami SS. Mechanical behaviour of reconstructed defected skull with custom PEEK implant and Titanium fixture plates under dynamic loading conditions using FEM. J Mech Behav Biomed Mater. 2023 Oct 1;146.

30. Carpenter RD, Klosterhoff BS, Torstrick FB, Foley KT, Burkus JK, Lee CSD, et al. Effect of porous orthopaedic implant material and structure on load sharing with simulated bone ingrowth: A finite element analysis comparing titanium and PEEK. J Mech Behav Biomed Mater. 2018 Apr 1;80:68–76.

31. Jindal P, Bharadwaja SSS, Rattra S, Chaitanya S, Gupta V, Breedon P, et al. Designing cranial fixture shapes and topologies for optimizing PEEK implant thickness in cranioplasty. Proceedings of the Institution of Mechanical Engineers, Part L: Journal of Materials: Design and Applications. 2023 Aug 1;237(8):1752–70.

32. Fournier M, Combès B, Roberts N, Braga J, Prima S. Mapping the distance between the brain and the inner surface of the skull and their global asymmetries. In: Medical Imaging 2011: Image Processing. SPIE; 2011. p. 79620Y.

33. Peters BJ. Practical Pin Tooling [Internet] [Master's Thesis]. Massachusetts Institute of Technology; 2013 [cited 2024 Dec 9]. Available from: http://hdl.handle.net/1721.1/100891

34. Jindal S, Manzoor F, Haslam N, Mancuso E. 3D printed composite materials for craniofacial implants: current concepts, challenges and future directions. Available from: https://doi.org/10.1007/s00170-020-06397-1

35. Ridwan-Pramana A, Marcián P, Borák L, Narra N, Forouzanfar T, Wolff J. Structural and mechanical implications of PMMA implant shape and interface geometry in cranioplasty – A finite element study. Journal of Cranio-Maxillofacial Surgery. 2016 Jan;44(1):34–44.

36. Marcián P, Narra N, Borák L, Chamrad J, Wolff J. Biomechanical performance of cranial implants with different thicknesses and material properties: A finite element study. Comput Biol Med. 2019 Jun;109:43–52.

37. ANSYS. Defining Bolt Preload [Internet]. ANSYS Innovation Space; 2020 [cited 2024 Dec 9]. Available from: https://innovationspace.ansys.com/courses/wp-content/uploads/sites/5/2020/10/2.2.2_Defining-Bolt-Preload_new_brand.pdf

38. Biewener AA. Safety factors in bone strength. Calcif Tissue Int. 1993 Feb;53(1 Supplement).

39. Yunkang Sui, Xirong Peng. Modeling, Solving and Application for Topology Optimization of Continuum Structures: ICM Method Based on Step Function [Internet]. Elsevier Butterworth-Heinemann; 2018 [cited 2024 Dec 10]. Available from: https://www.sciencedirect.com/topics/engineering/structural-topology-optimization

40. Pereira JT, Fancello EA, Barcellos CS. Topology optimization of continuum structures with material failure constraints. Vol. 26, Structural and Multidisciplinary Optimization. 2004. p. 50–66.

41. Bendsøe MP. Optimization of Structural Topology, Shape, and Material. Berlin, Heidelberg: Springer Berlin Heidelberg; 1995

42. Bendsøe MP, Kikuchi N. Generating optimal topologies in structural design

using a homogenization method. Comput Methods Appl Mech Eng [Internet]. 1988 Nov [cited 2024 Dec 9];71(2):197–224. Available from: https://linkinghub.elsevier.com/retrieve/pii/004578258890086240. Bendsùe MP, Sigmund O. Material interpolation schemes in topology optimization.

43. Bendsøe MP, Sigmund O. Material interpolation schemes in topology optimization. Archive of Applied Mechanics (Ingenieur Archiv) [Internet]. 1999 Nov 22;69(9–10):635–54. Available from:http://link.springer.com/10.1007/s004190050248

44. Duysinx P, Bendsøe MP. Topology optimization of continuum structures with local stress constraints. Int J Numer Methods Eng [Internet]. 1998 Dec 30;43(8):1453–78. Available from: https://onlinelibrary.wiley.com/doi/10.1002/(SICI)1097-0207(19981230)43:8<1453::AID-NME480>3.0.CO;2-2

45. Sved G, Ginos Z. Structural optimization under multiple loading. Int J Mech Sci. 1968 Oct;10(10):803–5.

46. Cheng GD, Guo X. ε -relaxed approach in structural topology optimization. Structural Optimization [Internet]. 1997 Jun;13(4):258–66. Available from: http://link.springer.com/10.1007/BF01197454

47. Kirsch U. On singular topologies in optimum structural design. Structural Optimization. 1990 Sep;2(3):133–42.

48. Lee JH, Frias V, Lee KW, Wright RF. Effect of implant size and shape on implant success rates: A literature review. J Prosthet Dent [Internet]. 2005 Oct;94(4):377–81. Available from: https://linkinghub.elsevier.com/retrieve/pii/S002239130500243X

49. Gutwald R, Jaeger R, Lambers FM. Customized mandibular reconstruction plates improve mechanical performance in a mandibular reconstruction model. Comput Methods Biomech Biomed Engin. 2017 Mar 12;20(4):426–35.

50. Antoniac IV, Stoia DI, Ghiban B, Tecu C, Miculescu F, Vigaru C, et al. Failure analysis of a humeral shaft locking compression plate-surface investigation and simulation by finite element method. Materials. 2019;12(7).